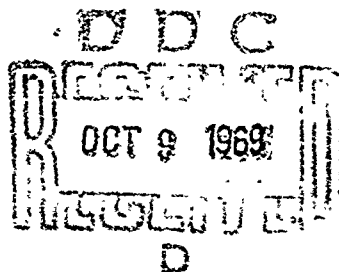


AD 694469

NOLTR 69-80

HOW TO ANALYZE 2-D SCHLIEN
PHOTOGRAPHS TO OBTAIN THE DENSITY
GRADIENT STRUCTURE OF 3-D FLOW FIELDS

By
Allen E. Winkelmann
Robert H. Feldhuhn



NOL

15 APRIL 1969

UNITED STATES NAVAL ORDNANCE LABORATORY, WHITE OAK, MARYLAND

NOLTR 69-80

ATTENTION

This document has been approved for
public release and sale, its distribution
is unlimited.

NOLTR 69-80

HOW TO ANALYZE 2-D SCHLIEREN
PHOTOGRAPHS TO OBTAIN THE DENSITY
GRADIENT STRUCTURE OF 3-D Flow Fields

Prepared by:
Allen E. Winkelmann
and Robert H. Feldhuhn

ABSTRACT: A technique is outlined by which density gradients visible in two-dimensional schlieren photographs can be analyzed to obtain the density gradient structure (i.e., the shape and location of density gradients such as shock waves and vortices, of three-dimensional flow fields. Practical application of the technique relies on obtaining a series of schlieren photographs of the flow field from different viewing orientations. The analysis is specialized to the case of a right-circular cone at angle of attack. Results are presented which show the shape and location of the bow shock of a 5° half-angle right-circular cone tested in the Supersonic Tunnel No. 2 at the U. S. Naval Ordnance Laboratory, White Oak, at a nominal Mach number of 5.0, a nominal free-stream Reynolds number per foot of 4.8×10^6 and angles of attack equal to 15° and 40° .

U. S. NAVAL ORDNANCE LABORATORY
WHITE OAK, MARYLAND

15 April 1969

How to Analyze 2-D Schlieren Photographs to Obtain the Density Gradient Structure of 3-D Flow Fields

In this report, a technique is outlined by which density gradients visible in two-dimensional schlieren photographs can be analyzed to obtain the density gradient structure of three-dimensional flow fields. The analysis is specialized to the case of a right-circular cone at angle of attack. Results are presented which show the shape and location of the bow shock on a 5° half-angle cone at a Mach number of 5 and angles of attack of 15° and 40° .

The work described in this report has been sponsored by the Advanced Research Projects Agency under ARPA order number 905 Program Code No. 6E30 as part of Project DEFENDER.

E. F. SCHREITER
Captain, USN
Commander

L. H. Schindel
L. H. SCHINDEL
Aerodynamics Department

CONTENTS

	Page
INTRODUCTION.	1
GENERAL APPROACH - ARBITRARY BODY AT ANGLE OF ATTACK.	1
Basic Concept of the Analysis	1
Extension of Basic Concept to General Case.	2
Development of Equation for "Effective Line of Sight"	3
Concluding Comments on the General Approach	5
SPECIAL CASE - THE RIGHT-CIRCULAR CONE AT ANGLE OF ATTACK	5
Basic Geometry and Definitions.	5
Determination of $f(y)$ - The Functional Form of the Density Gradient	6
Equation of "Effective Line of Sight"	7
Construction of "Effective Lines of Sight" in the Cross-Sectional Plane.	8
RESULTS OF THE ANALYSIS OF A RIGHT-CIRCULAR CONE AT ANGLE OF ATTACK.	9
Obtaining the Schlieren Photographs	9
Shape of the Bow Shock.	9
Errors.	10
SUMMARY	10

REFERENCES

1. Feldhuhn, Robert H. and Winkelmann, Allen E., "Separated Flow Phenomena on a Slender Cone at Mach 5," NOLTR 69-36, 1969
2. Larcombe, M. J., "Estimation of Surface Pressures From Observed Shock-Wave Envelopes Surrounding Conical Bodies at $M = 4.0$," NPL Aero Report 1244, August 1967

ILLUSTRATIONS

Figure

- 1 2-D Schlieren View of a 3-D Flow Field About an Arbitrary Body
- 2a,b Cross-Sectional Planes at Various Roll Angles φ , and Their Projections onto the Schlieren Photograph
- 3 Geometry of General Case - Arbitrary Body at Angle of Attack
- 4 Construction in Plane Q of the Shape and Location of Density Gradients
- 5a Schlieren Photograph of a 5° Half-Angle Cone at Angle of Attack of 40° , $\varphi = 0^\circ$
- 5b $\varphi = 60^\circ$
- 5c $\varphi = 90^\circ$
- 6 Wind Tunnel - Schlieren Arrangement for Viewing Cone at Varying Orientations of Roll Angle φ
- 7 Geometry of Schlieren Photographs of a Right-Circular Cone at Angle of Attack
- 8 Geometry for Relation Between l and d
- 9 Geometry of Polar Transformation
- 10 Construction of "Effective Line of Sight" in Polar Cross-Sectional Plane
- 11a Schlieren Photograph of a 5° Half-Angle Cone at Angle of Attack of 15° , $\varphi = 0^\circ$
- 11b $\varphi = 60^\circ$
- 11c $\varphi = 90^\circ$
- 12 Shock-Wave Profile of Right-Circular Cone at Angle of Attack, $\alpha = 15^\circ$
- 13 Shock-Wave Profile of Right-Circular Cone at Angle of Attack, $\alpha = 40^\circ$

NOMENCLATURE

d	diameter
l	measurement taken along the cone axis, from the tip to the location of the "s" measurement
\bar{n}	normal to cross-sectional plane Q
r	radial distance along a ray in the polar cross-sectional plane
s	measurement taken perpendicular to the cone axis, from the axis to a density gradient
$O(x_0, y_0, z_0)$	origin of the (x', y', z') body fixed-coordinate system
(o, y_0'', z_0'')	origin of the (x'', y'', z'') tip fixed-coordinate system on the cone
x_n, y_n, z_n	components of normal vector \bar{n}
(x, y, z)	schlieren (tunnel fixed) coordinate system
(x', y', z')	body fixed-coordinate system
(x'', y'', z'')	tip fixed-coordinate system
α	angle of attack of the reference axis to the free stream
α_a	apparent angle of attack of the cone in the schlieren photograph - measured positive in a counter-clockwise direction from the positive z axis, $\alpha_a = \tan^{-1}(\cos\phi \tan\alpha)$
θ_c	half angle of cone
ϕ	roll angle of cone "dog leg" sting plane
λ	angular position in polar cross-sectional plane Q

Other symbols are defined in the text where they appear.

INTRODUCTION

The conventional two-dimensional schlieren system is widely used in aerodynamic research to locate density gradients occurring in a flow field. A typical example is the shock wave formed on a two-dimensional wedge in supersonic flow. Schlieren photographs of an essentially two-dimensional flow field are relatively easy to interpret because every plane parallel to the schlieren plane can be considered as similar. Schlieren photographs of a three-dimensional flow field (e.g., a cone at angle of attack) are more difficult to interpret because, in general, planes parallel to the schlieren plane are not similar (Fig. 1).

Holographic techniques, combined with the schlieren principle, promise to provide a means to locate density gradients in their true three-dimensional perspective. However, a technique is presented in this report by which density gradients visible to a conventional two-dimensional schlieren system can be analyzed to obtain the density gradient structure (i.e., the shape and location of density gradients, such as shock waves and vortices) of a three-dimensional flow field.

In the sections to follow, this technique is developed for the general case of an arbitrary body at angle of attack. As a special example, the results of an analysis of a right-circular cone at angle of attack are presented.

GENERAL APPROACH - ARBITRARY BODY
AT ANGLE OF ATTACK

Basic Concept of the Analysis

A two-dimensional schlieren photograph of a three-dimensional flow field about an arbitrary body will generally show density gradients as curved lines or regions (Fig. 1). The density gradient structure in a cross-sectional plane, AA, is depicted in Figure 2.

The schlieren light path (parallel to the x axis of the schlieren (tunnel fixed) coordinate system (x,y,z)) will be referred to in this report as the schlieren "line of sight." A projection along "lines of sight" of the body and regions of density gradients produces the image on the schlieren plane (Fig. 1). It is important to note that a density gradient occurs someplace along the "line of sight," and not necessarily directly above or below the body as the schlieren photographs would seem to suggest (this will be illustrated subsequently). In this report, the projection or image of a density gradient on a schlieren photograph will be referred to merely as the density gradient in the photograph.

Large density gradients may occur in the form of surfaces (e.g., shock waves) or "line sources" (e.g., vortices). In turn, these density gradients may appear as diffuse images (e.g., the vortices in Fig. 2) or very distinct images (e.g., the bow shock in Fig. 2) in the schlieren photograph. "Lines of sight" are shown to pass through the center of the vortices. Considering the bow shock to be of infinitesimal thickness, the "lines of sight" run tangent to the bow shock (Fig. 2).

A reference axis is defined to coincide with the tunnel axis (parallel to the flow direction) for convenience of illustration; however, in general, the reference axis has an arbitrary orientation. The origin of a body fixed coordinate system (x', y', z') is located in cross-sectional plane AA, with z' along the reference axis, and x' parallel to x when the body has not been rolled about the tunnel axis. If the body is rolled about the tunnel axis an angle ϕ (a sting mounted in a roll head of a wind tunnel allows the model to roll while maintaining the same angle of attack to the flow), the schlieren photograph presents a new image as seen by comparing Figures 2a and 2b. The superposition of a number of cross-sectional planes taken at varying roll angles ϕ , would show the center of the vortices to be regions of intersecting "lines of sight" while the bow shock would be defined by an envelope of "lines of sight" in the (x', y') plane. By using a series of cross-sectional planes taken along the reference axis, the entire density gradient structure of the three-dimensional flow field could be constructed in detail. Obviously, any density gradient structure always hidden from view by an opaque body, or that is too weak to be photographed, cannot be constructed by using the analysis of this report.

The above presents the basic concept behind the technique presented in this report. The next step will be to extend this concept to the more complex geometry of the general three-dimensional flow field about an arbitrary body.

Extension of Basic Concept to General Case

The geometry for the general three-dimensional flow field about an arbitrary body (only the reference axis, RF , is shown) is shown in Figure 3. The reference axis, RF , is at angle of attack, α , to the free stream, and lies in a plane which is rolled about the tunnel axis (parallel to the free-stream flow direction) an angle ϕ ($\phi = 0^\circ$ corresponding to the case when the reference axis lies in a plane parallel to the schlieren plane). The projection of the reference axis (along the schlieren "line of sight") onto the schlieren plane (y, z) is indicated by line MG . A curved shock wave is assumed to exist in the flow field. A curved surface A , made up of "lines of sight" tangent to the shock wave along line TN , intersects the schlieren plane in line SP . Line SP is what appears as a density gradient in the schlieren photograph. A cross-sectional

plane, Q, perpendicular to the reference axis at point O, is intersected by surface A along line CD. A body fixed-coordinate system (x',y',z') , with origin at point O, is oriented with the x' axis parallel to the x axis of the schlieren (tunnel fixed) coordinate system (x,y,z) when $\phi = 0^\circ$.

Analogous to the special case of Figure 2, a superposition of cross-sectional planes Q (obtained at a series of roll angles, ϕ) will define the shock wave by an envelope of CD lines in the (x',y') plane (Fig. 4). In the special case of Figure 2, the envelope is defined by "lines of sight." However, CD lines are the loci of points of intersection of a series of "lines of sight" with plane Q (i.e., the intersection of surface A and plane Q). For the remainder of this report, CD lines will be referred to as "effective lines of sight." In general, "effective lines of sight" will be curved and density gradients will occur someplace along these lines.

Had a vortex been considered to exist in Figure 3, a series of intersecting "effective lines of sight" would define its center (Fig. 4). Once the shape and location of the density gradients have been established, the cross-sectional shape of the body can be added to complete the picture. The entire density gradient structure of the three-dimensional flow field could be constructed using a series of cross-sectional planes located along the reference axis.

The next step will be to determine the necessary equations to construct an "effective line of sight" from a given equation for a density gradient, SP.

Development of Equations for "Effective Line of Sight"

Basically, the analysis consists of finding equations in the (x',y',z') system which define the line of intersection, CD, of surface A with plane Q. The details of this analysis are presented below.

a. Surface A

The functional form of surface A in the (x,y,z) system is:

$$A(x,y,z) = 0 \quad (1)$$

and after transformation to the (x',y',z') system:

$$A'(x',y',z') = 0 \quad (2)$$

More explicitly, surface A is related to the functional form of the density gradient, SP, in the schlieren plane:

$$z = f(y) \quad (3)$$

b. Plane Q

The functional form of plane Q in the (x,y,z) system is:

$$Q(x,y,z) = 0 \quad (4)$$

and a transformation to the (x',y',z') system together with z' = 0 in the Q plane gives:

$$Q'(x',y',z') = 0 \quad (5)$$

Plane Q is defined by its normal

$$\bar{n} = x_n \bar{i} + y_n \bar{j} + z_n \bar{k} \quad (6)$$

and point O(x₀,y₀,z₀). Hence the explicit form of equation (4) becomes:

$$x_n(x-x_0) + y_n(y-y_0) + z_n(z-z_0) = 0 \quad (7)$$

The transformation equations necessary to determine equation (5) are found with the aid of Figure 3 to be:

$$\begin{aligned} x &= x_0 + x' \cos \varphi - y' \cos \alpha \sin \varphi - z' \sin \alpha \sin \varphi \\ y &= y_0 + x' \sin \varphi + y' \cos \alpha \cos \varphi + z' \sin \alpha \cos \varphi \\ z &= z_0 - y' \sin \alpha + z' \cos \alpha \end{aligned} \quad (8)$$

and the normal to plane Q, which is parallel to the z' axis, is:

$$\bar{n} = -\sin \alpha \sin \varphi \bar{i} + \sin \alpha \cos \varphi \bar{j} + \cos \alpha \bar{k} \quad (9)$$

c. "Effective line of sight," CD

The intersection of surface A and plane Q defines the "effective line of sight," CD. Expressed functionally in the (x',y',z') system, the equation of line CD is:

$$y' = g(x') \quad (10)$$

Substitution of equation (3) into equation (7), together with equations (8) and (9), gives the explicit form of equation (10), and hence the equation of the "effective line of sight" as:

$$y' = \frac{z_0 - f(y)}{\sin \alpha} \quad (11)$$

The functional form, f(y), is retained in equation (11) but would in practice, be transformed through equation (8) to a function

of (x',y') . The value of z_0 , which is a constant for the geometry of Figure 3, serves to specify the cross-sectional plane under construction.

Concluding Comments on the General Approach

The use of a reference axis and a cross-sectional plane perpendicular to the axis will be the most convenient in the majority of body shapes, such as cones, lifting bodies, etc. However, in principle, other geometrical arrangements may be used for specific applications. For sting supported models, the reference axis can be taken along the sting when it is visible in the schlieren photographs. In practice, data measurements would be referenced to the origin of the (x,y,z) system and curve fitting would yield equations of the form $(z = f(y))$ describing the density gradients. The images of shock waves are generally very distinct lines and can be described by single equations. However, diffuse images may require several equations to properly define the region of the density gradient. In some cases, data may be referenced to a point on the projected reference axis, as to be shown in the next section where the projection of the tip of the cone is chosen as the reference point. The value for z_0 is easily obtained from a schlieren photograph showing the reference axis in true length (e.g., when $\phi = 0^\circ$).

Finally, it is conceivable that the geometric analysis presented above could be extended for use with shadowgraph and interferometer systems.

SPECIAL CASE - THE RIGHT-CIRCULAR CONE AT ANGLE OF ATTACK

In this section the general result of equation (11) is specialized to an analysis of two-dimensional schlieren photographs of a right-circular cone at angle of attack.

For a given configuration, the terms z_0 and $\sin\alpha$ are constant in equation (11). Hence, one merely needs to determine the proper form of $f(y)$, which describes the density gradient in the schlieren photograph.

Before determining the functional form $f(y)$ for density gradients about a circular cone at angle of attack, the basic geometry must be defined.

Basic Geometry and Definitions

A series of schlieren photographs of a cone at angle of attack is shown in Figures 5a, b, and c. The density gradients appearing in these photographs seem to emanate from the image (projection onto the schlieren plane) of the cone tip and are essentially straight lines (suggesting that the flow around the cone is essentially

conical). Hence, for the purpose of this analysis the images of these density gradients are assumed to be straight lines emanating from tip.

A schematic in Figure 6 depicts the wind-tunnel schlieren photographic arrangement and defines the roll angle, ϕ , of a cone mounted on a "dog leg" sting. For this geometry the reference axis is defined to coincide with the cone axis. Obviously, the cross-sectional plane perpendicular to the reference axis (referred to hereafter as the cone axis) shows the cross section of the cone as a circle.

In Figure 7 the geometry of a typical schlieren photograph is shown. The image of the cone and sting defines the projected cone axis and tip. For the purposes of data measurements, the reference point is chosen as the origin (o, y_0, z_0) of a tip fixed-coordinate system (x, y, z).

The basic data taken with each photograph consisted of:

- α - angle of attack of the cone to the free stream
- ϕ - roll angle of cone-"dog leg" sting plane
- θ_c - half angle of cone
- α_a - apparent angle of attack of cone in schlieren photograph - measured positive in a counterclockwise direction from the positive z axis
 $\alpha_a = \tan^{-1} (\cos \phi \tan \alpha)$
- s - measurement taken perpendicular to the projected cone axis, from the axis to a density gradient
- l - measurement taken along the projected cone axis from the tip to the location of the "s" measurement

In the equations to be developed below s and l appear as a ratio, l/s . Hence, the location of the measurement of s and l is arbitrary by consequence of similar triangles (Fig. 7). This implies that all cross-sectional planes along the cone axis present a similar density gradient profile. For convenience of discussion, the measurement of s is taken at point (o, y_0, z_0) in Figure 7.

Determination of $f(y)$ - The Functional Form of the Density Gradient

It is convenient to refer to density gradients as occurring "above" or "below" the projected cone axis according to their relation to the (x, y, z) system (Fig. 7).

The equation of a density gradient occurring "above" the axis in Figure 7 has the form:

$$z'' = -\frac{l}{s} y'' \quad (12a)$$

The equation of a density gradient occurring "below" the axis has the form:

$$z'' = \frac{l}{s} y'' \quad (12b)$$

The next step is to transform equation (12a) and (12b) to the (x,y,z) system to obtain the functional form $z = f(y)$. The transformation of equation (12a) will be shown in detail below.

The appropriate transformation relations are:

$$\begin{aligned} x'' &= x \\ y'' &= (y-y_0'')\cos\alpha_a - (z-z_0'')\sin\alpha_a \\ z'' &= (y-y_0'')\sin\alpha_a + (z-z_0'')\cos\alpha_a \end{aligned} \quad (13)$$

Upon substitution of equation (13) into equation (12a) we have:

$$z = f(y) = z_0'' - (y-y_0'')E_a \quad (14)$$

where

$$E_a = \frac{\sin\alpha_a + \frac{l}{s}\cos\alpha_a}{\cos\alpha_a - \frac{l}{s}\sin\alpha_a} \quad (15)$$

A similar form for equation (12b) is found by replacing E_a in equation (14) by:

$$E_b = \frac{\sin\alpha_a - \frac{l}{s}\cos\alpha_a}{\cos\alpha_a + \frac{l}{s}\sin\alpha_a} \quad (16)$$

Equation of "Effective Line of Sight"

Because a density gradient appearing about the cone in the schlieren photograph is essentially a straight line, surface A of the general approach is now a plane. Hence, the "effective line of sight," defined by the intersection of plane A and plane Q, is a straight line. The equation of this line is developed below.

Applying equation (8) and (14) to equation (11), results in

$$y'\sin\alpha = (z_0 - z_0'') + (y_0 - y_0'' + x'\sin\phi + y'\cos\alpha \cos\phi)E_a \quad (17)$$

From Figure 7 we see that:

$$\begin{aligned} y_0 - y_0'' &= -l \sin \alpha_a \\ z_0 - z_0'' &= -l \cos \alpha_a \end{aligned} \quad (18)$$

which, after non-dimensionalizing by the cone diameter, d , at point O , brings equation (17) to:

$$\frac{y'}{d} \sin \alpha = -\frac{l}{d} \cos \alpha + \left[-\frac{l}{d} \sin \alpha + \frac{x'}{d} \sin \varphi + \frac{y'}{d} \cos \alpha \cos \varphi \right] E_a \quad (19)$$

As the cone is rolled through angles φ , the relationship between l and d varies. This is taken into account by a geometrical consideration shown in Figure 8, with the result that:

$$\frac{l}{d} = \frac{\cos \alpha}{2 \tan \theta_c \cos \alpha_a} \quad (20)$$

Application of equation (20) yields the equation for the "effective line of sight" in the (x', y', z') system:

$$\frac{y'}{d} = \frac{\frac{x'}{d} E_a \sin \varphi - \frac{\cos \alpha}{2 \tan \theta_c} \left[1 + E_a \tan \alpha_a \right]}{\sin \alpha - E_a \cos \alpha \cos \varphi} \quad (21)$$

A similar equation is found for density gradients appearing "below" the projected cone axis where E_a is replaced by E_b in equation (21).

Construction of "Effective Lines of Sight" in the Cross-Sectional Plane

It was found convenient to present the results of the analysis of the cone in a polar diagram representing the cross-sectional plane Q . Using the relations defined in Figure 9, equation (21) for density gradients appearing "above" the projected cone axis, becomes:

$$\frac{r}{d} = \frac{\frac{\cos \alpha}{2 \tan \theta_c} \left[1 + E_a \tan \alpha_a \right]}{E_a \sin \lambda \sin \varphi - \cos \lambda \left[\sin \alpha - E_a \cos \alpha \cos \varphi \right]} \quad (22)$$

Replacing E_a by E_b yields a form for density gradients appearing "below" the axis. In applying equation (22) for the range $90^\circ < \varphi < 270$ degrees, it must be noted that α_a is a negative angle.

NOLTR 69-80

The "effective line of sight" is a straight line and can be defined by two points calculated from equation (22) (Fig. 10). One point can be found by assuming for convenience, $\lambda_1 = \varphi$. A second point can be found along a ray rotated a convenient angle in either direction from r_1/d , to angular position λ_2 . Finally, the body shape is constructed as a circle of unit diameter about point O.

Because every cross-sectional plane along the cone axis is similar, one cross-sectional plane serves to define the density gradient structure of the flow field.

RESULTS OF THE ANALYSIS OF A RIGHT-CIRCULAR CONE AT ANGLE OF ATTACK

Obtaining the Schlieren Photographs

In this section, the results of applying the above technique to schlieren pictures of a cone at angle of attack are presented. Schlieren photographs used for analysis were obtained as part of a more extensive study of the flow field about an inclined right-circular cone conducted in the Supersonic Tunnel No. 2 at the U. S. Naval Ordnance Laboratory, White Oak (Ref. 1). Figures 5a, 5b, and 5c are typical of schlieren photographs obtained of a 5° half-angle right-circular cone at nominal free-stream Mach number of 5.0, a nominal free-stream Reynolds number per foot of 4.8×10^6 , and an angle of attack, $\alpha = 40^\circ$. Figures 11a, 11b, and 11c show a similar series at $\alpha = 15^\circ$. Photographs were taken in increments of roll, $\Delta\varphi = 10^\circ$ over the range $0^\circ < \varphi < 180^\circ$. Because of symmetry, the series from 0° to 90° was duplicated by the series from 90° to 180° . In addition to the "still" photographs, movies were taken of the cone continuously rolling from 0° to 180° . Although the latter provided many more views to analyze, the quality of definition was not as good as the "still" photographs.

Shape of the Bow Shock

The image of the bow shock appeared in the schlieren photographs as distinct lines and hence was described by single equations "above" and "below" the projected cone axis. The profiles of the bow shocks formed on the cone at angles of attack of $\alpha = 15^\circ$ and 40° are shown in the cross-sectional planes of Figures 12 and 13. Because all cross-sectional planes along the cone axis are similar, one plane serves to describe the shock shape for a given angle of attack.

The shock envelopes are shown not to be closed because the shock waves were too weak to be visible in the region of the leeward meridian. If these envelopes were to close, it appears that they would nearly coincide with the free-stream Mach wave projection on the leeward meridian.

The "effective lines of sight" calculated for $\varphi = 0^\circ$, 60° , and 90° are shown in Figure 13 for the case of $\alpha = 40^\circ$. It is interesting to note that the "effective line of sight" for $\varphi = 90^\circ$

defines a portion of the bow shock at approximately 45° from the leeward meridian. That is, the portion of the bow shock visible in Figure 5c does not lie directly above or below the cone (i.e., on a ray 90° from the leeward meridian) as the schlieren photograph would seem to suggest.

No attempt was made to compare the shock shapes of Figures 12 and 13 with analytical calculations. Furthermore, no flow surveys were completed to substantiate the location of the shock wave. Other density gradients appearing on the leeward side of the cone in Figures 5 and 11 are currently under investigation and the results of this study will be presented in a later report.

Errors

Errors introduced in obtaining the raw data can obviously be reduced by working from enlargements of the photographs. In the calculation of two points which define an "effective line of sight," sufficient accuracy of the line orientation was obtained by locating the points relatively far apart (i.e., rotating λ_2 relatively far from λ_1).

SUMMARY

A technique has been outlined by which the density gradients visible in two-dimensional schlieren photographs can be analyzed to yield the density gradient structure (i.e., the shape and location of density gradients such as shock waves and vortices) of a three-dimensional flow field. The analysis has been specialized to treat the case of a right-circular cone at angle of attack. Practical application of the technique has relied on obtaining a series of schlieren photographs of the flow field from different viewing orientations by rolling the model relative to the schlieren system. Results have been presented which show the shape and location of the bow shock formed on a 5° half-angle right-circular cone tested in the Supersonic Tunnel No. 2 at the U. S. Naval Ordnance Laboratory, White Oak, at a nominal Mach number of 5.0, a nominal free-stream Reynolds number of 4.8×10^6 , and angles of attack equal to 15° and 40° .

Since the completion of the work for this report, the authors have become aware of a similar technique for determining the shape of the bow shock around conical shapes as presented in Reference 2.

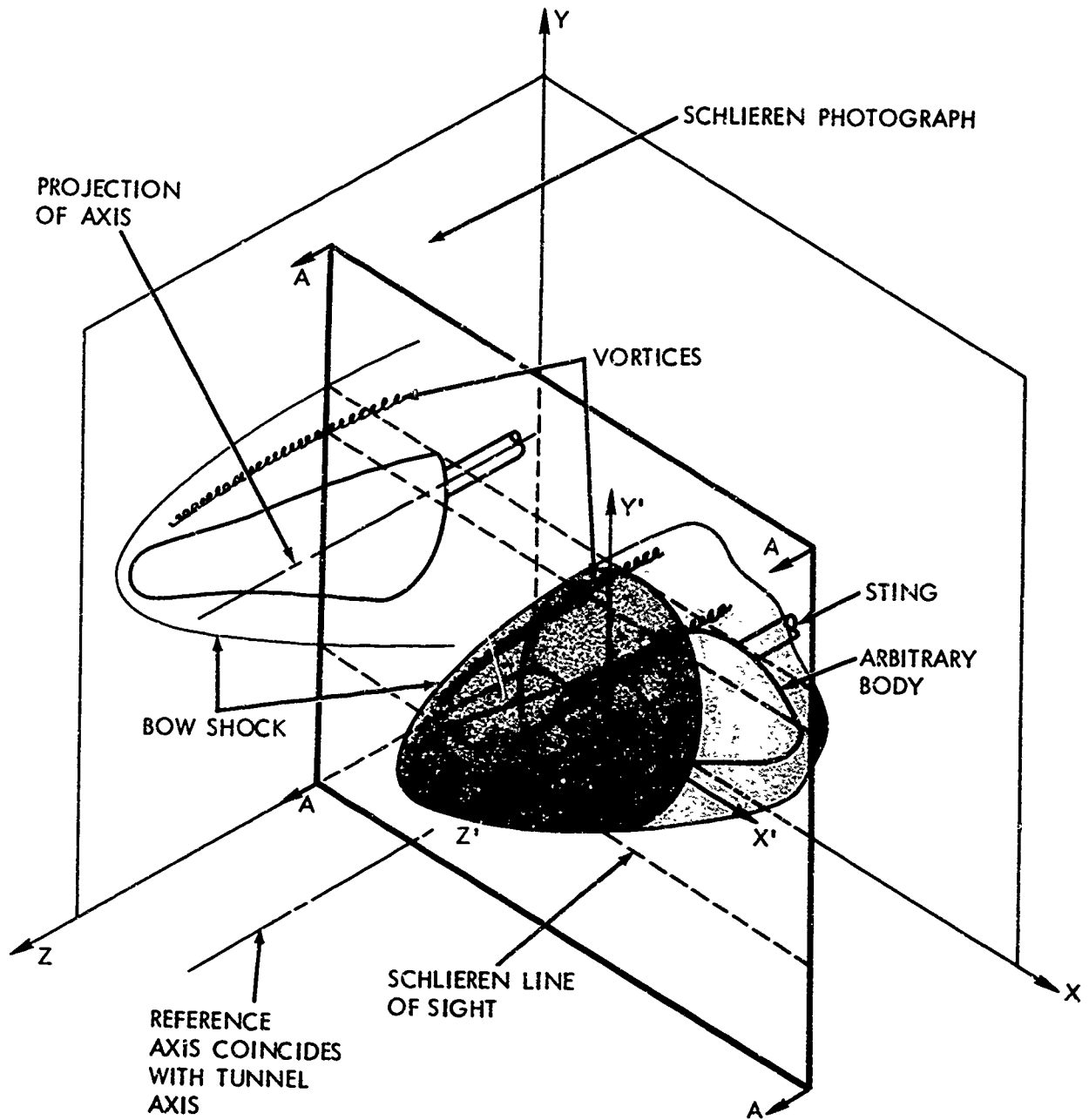
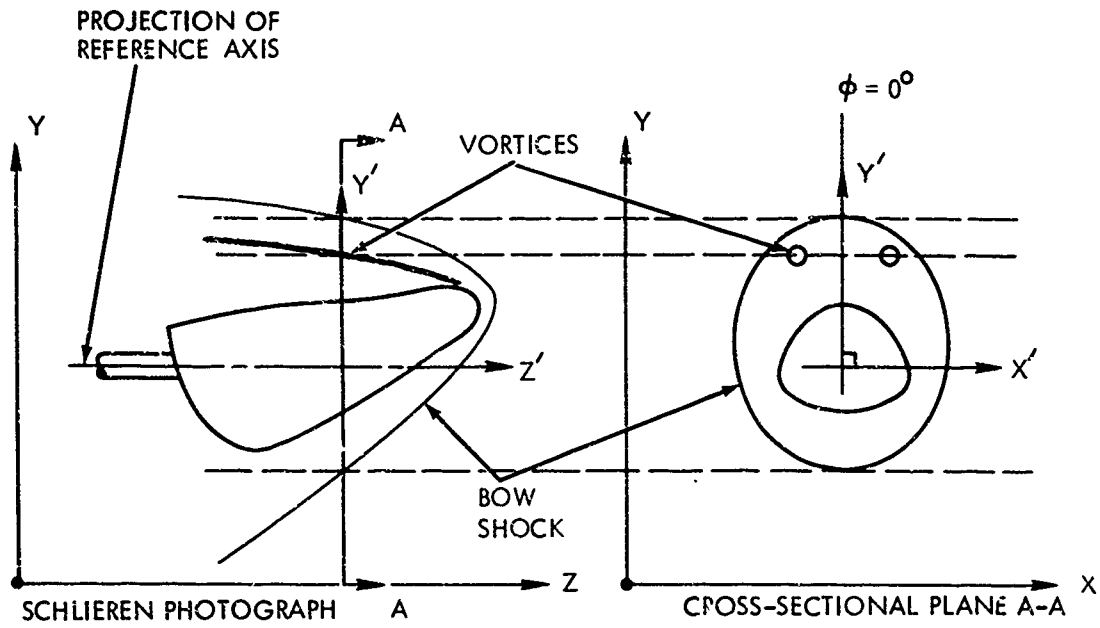
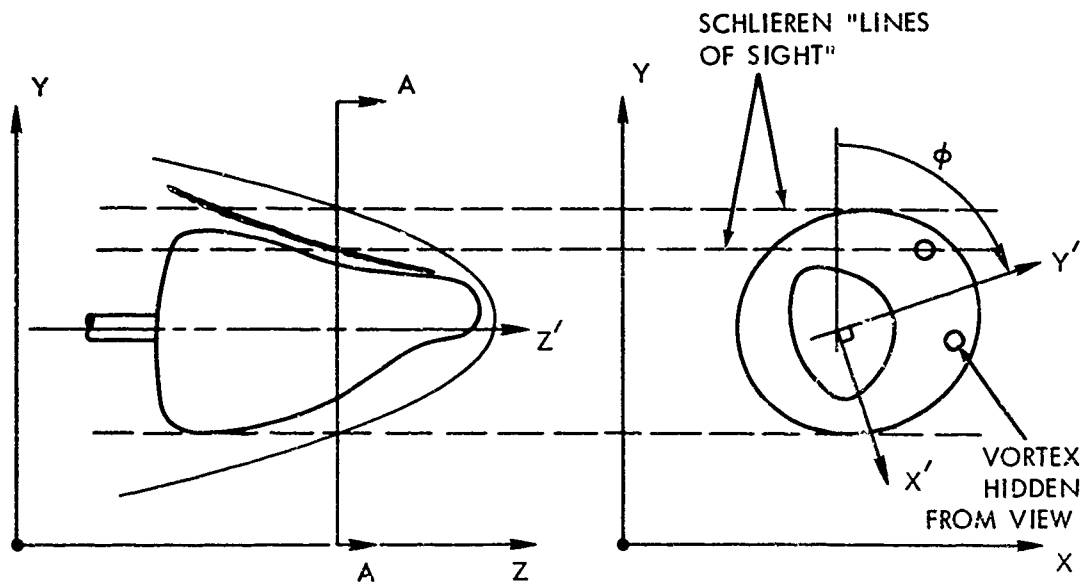


FIG. 1 2-D SCHLIEREN VIEW OF A 3-D FLOW FIELD ABOUT AN ARBITRARY BODY.



a. CROSS-SECTIONAL PLANE A-A WHEN $\phi = 0$



b. CROSS-SECTIONAL PLANE A-A WHEN $\phi > 0^\circ$

FIG. 2 CROSS-SECTIONAL PLANES AT VARIOUS ROLL ANGLES ϕ , AND THEIR PROJECTIONS ONTO THE SCHLIEREN PHOTOGRAPH

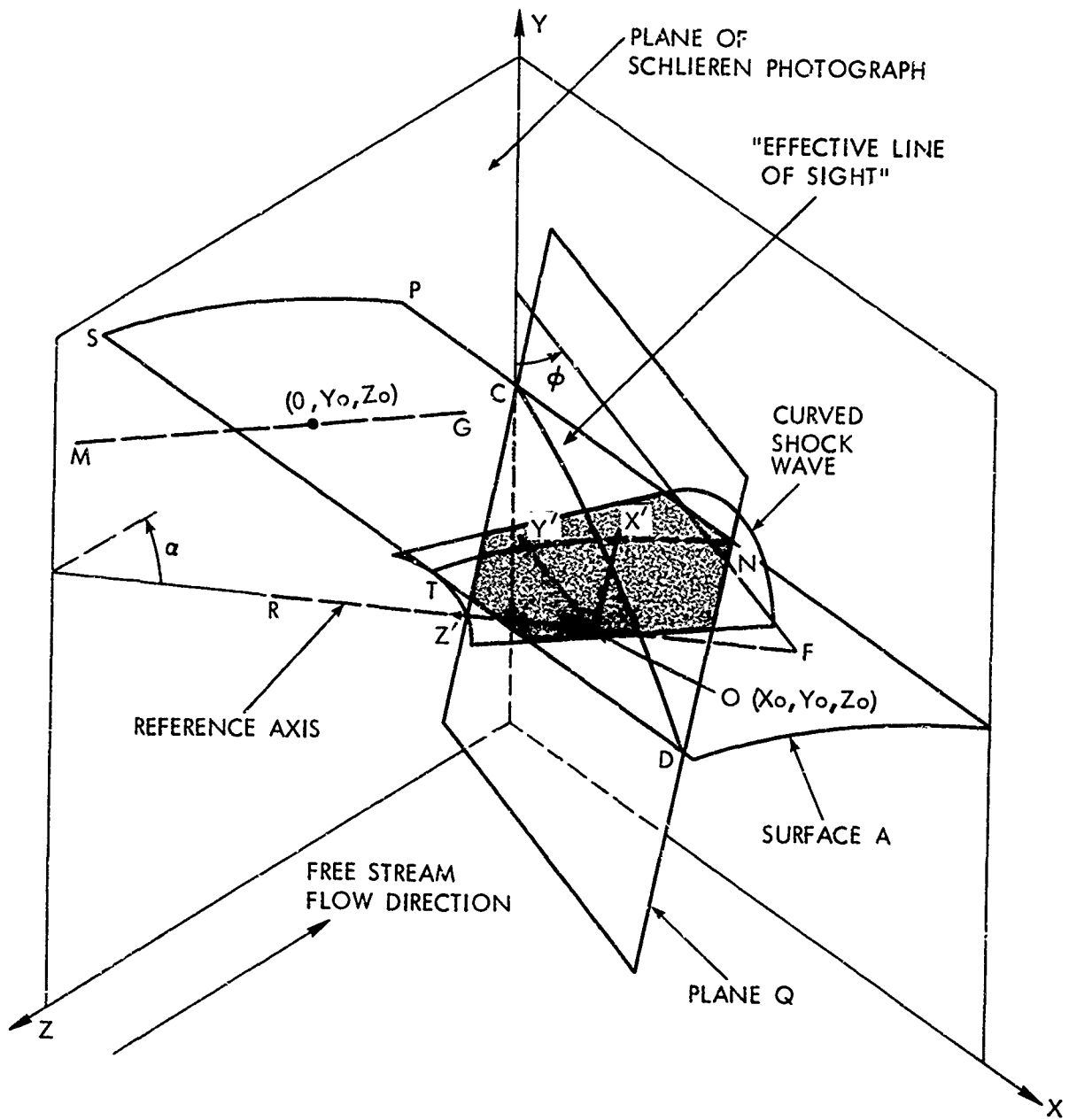


FIG. 3 GEOMETRY OF GENERAL CASE - ARBITRARY BODY AT ANGLE OF ATTACK

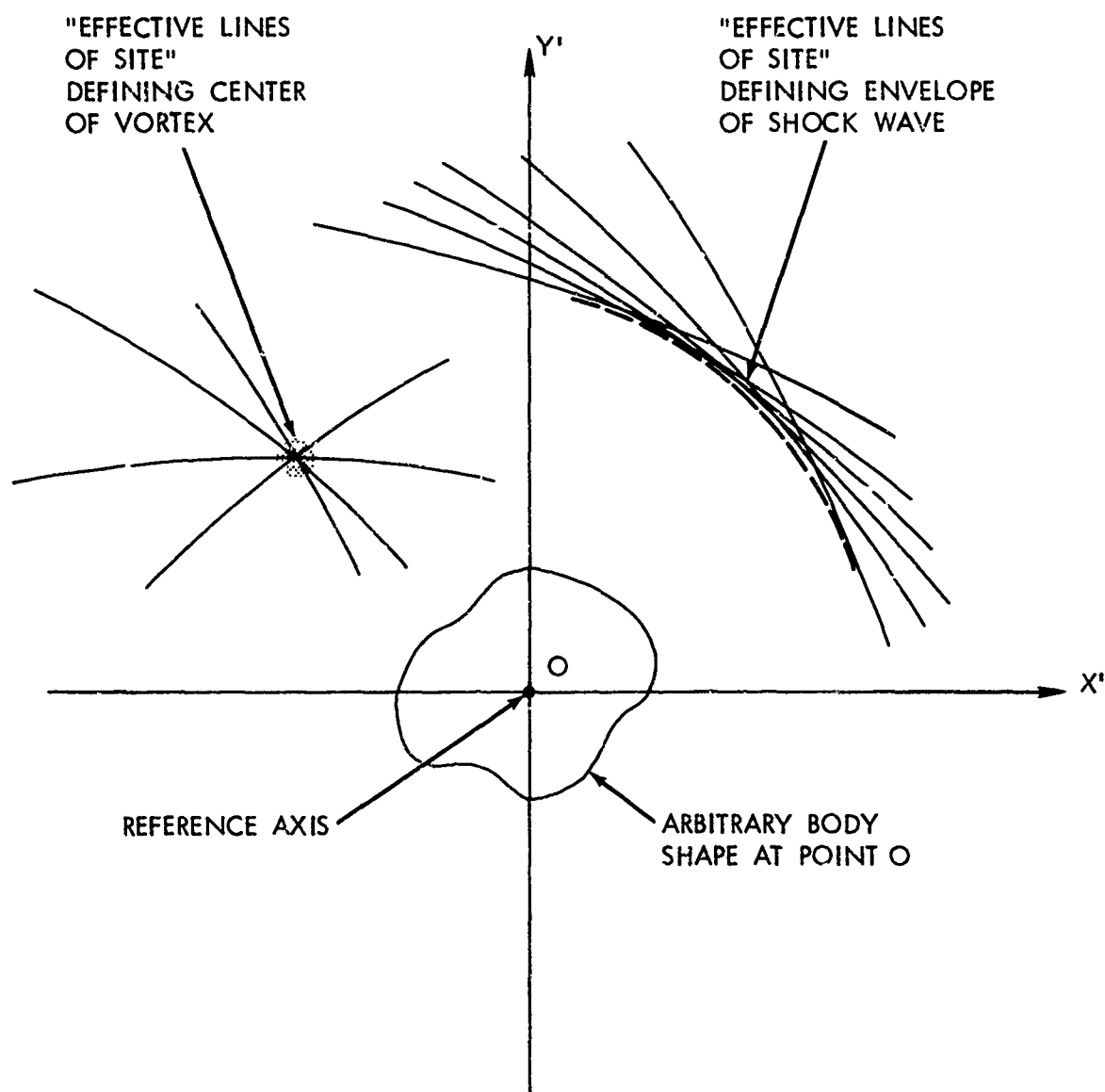


FIG. 4 CONSTRUCTION IN PLANE Q OF THE SHAPE AND LOCATION OF DENSITY GRADIENTS.

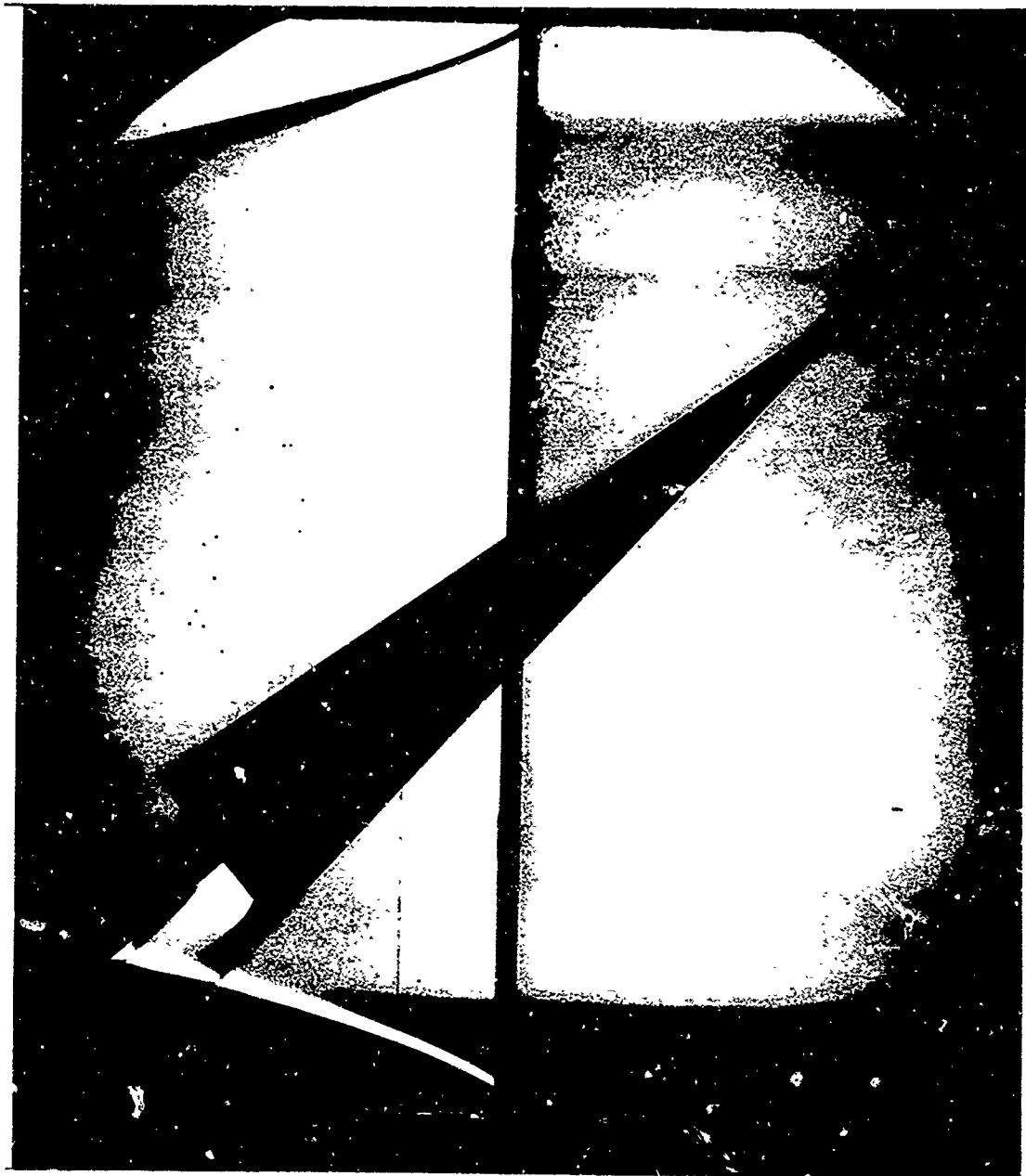


FIG. 5a SCHLIEREN PHOTOGRAPH OF A 5° HALF ANGLE CONE AT ANGLE OF ATTACK $\alpha = 40^\circ$, $\phi = 0^\circ$.



FIG. 5b $\phi = 60^\circ$

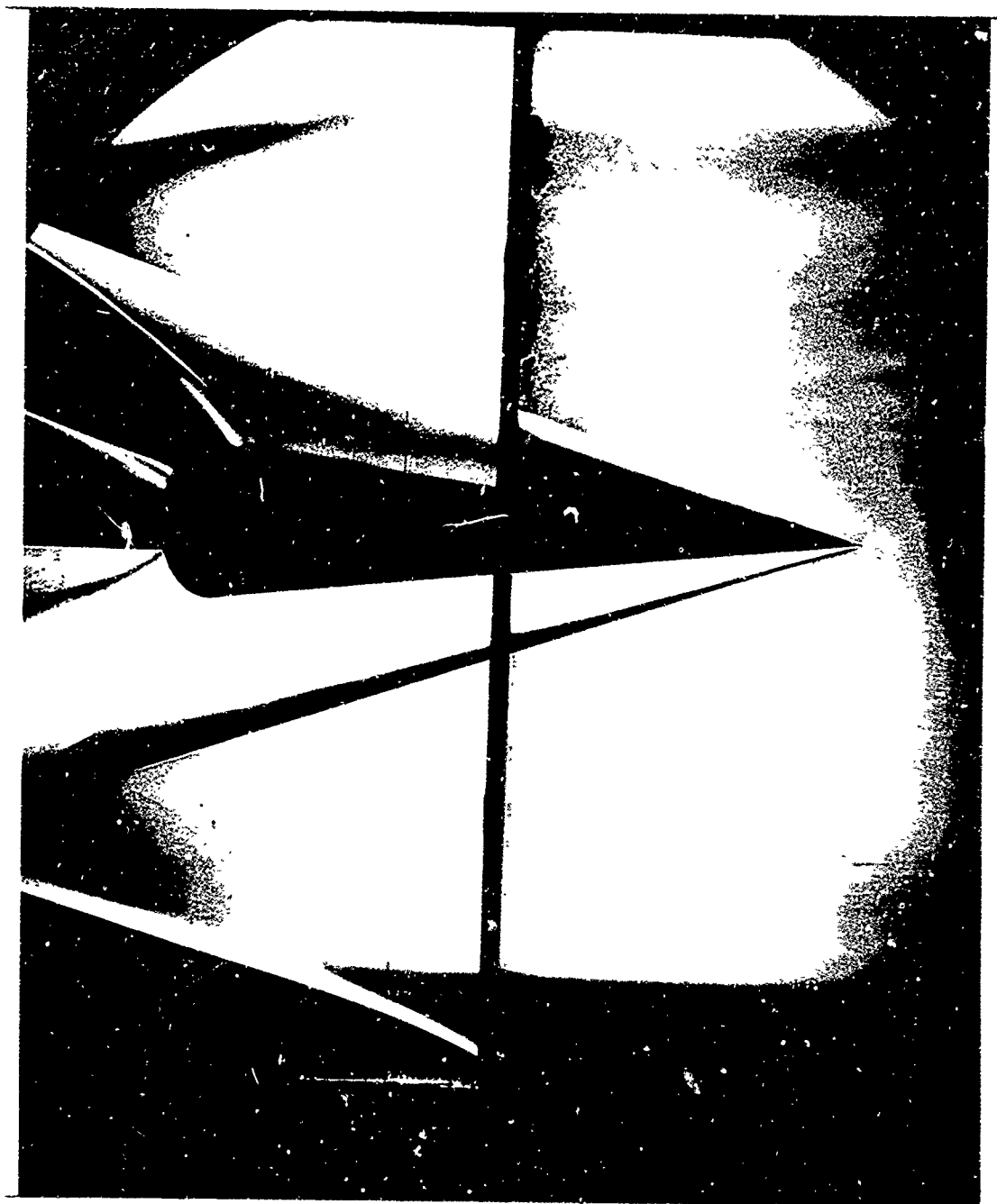


FIG. 5c $\phi = 90^\circ$

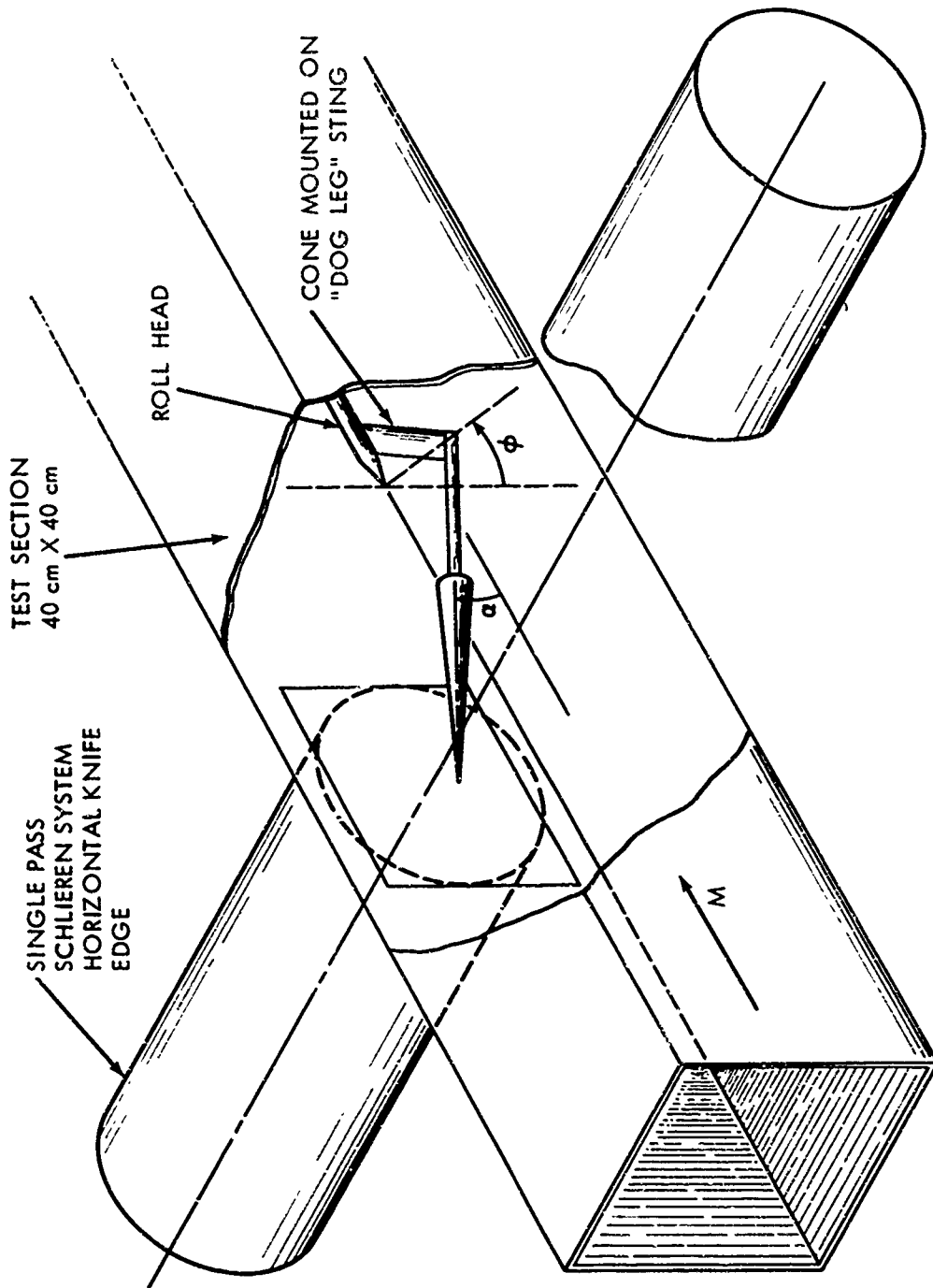


FIG. 6 WIND TUNNEL-SCHLIEREN ARRANGEMENT FOR VIEWING CONE AT VARYING ORIENTATIONS OF ROLL ANGLE ϕ

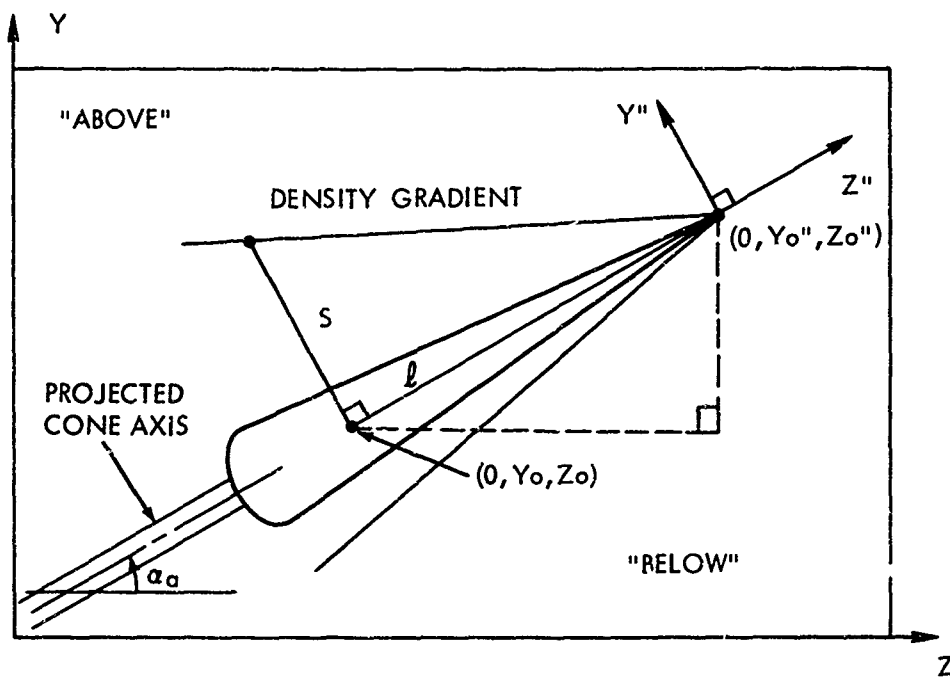


FIG. 7 GEOMETRY OF SCHLIEN PHOTOGRAPHS OF A RIGHT CIRCULAR CONE AT ANGLE OF ATTACK

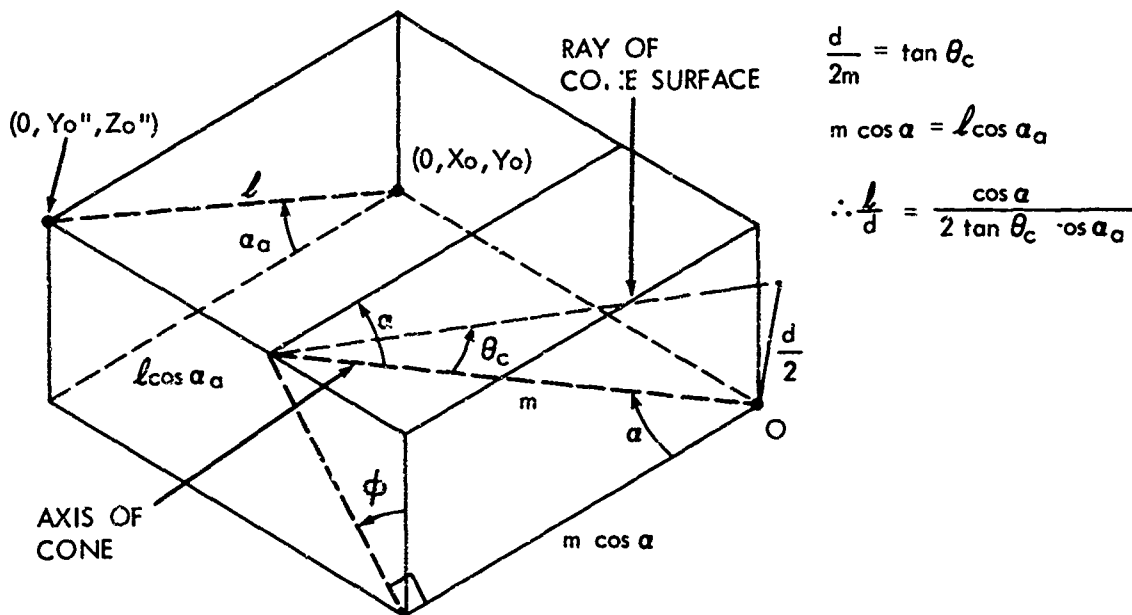


FIG. 8 GEOMETRY FOR RELATION BETWEEN l AND d

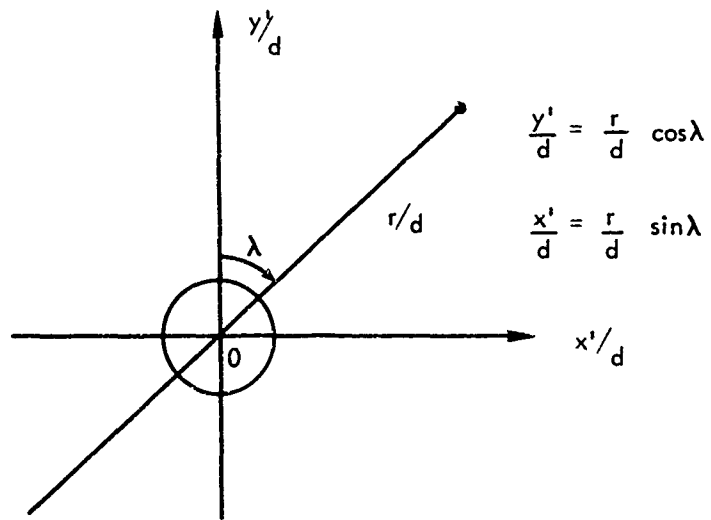


FIG. 9 GEOMETRY OF POLAR TRANSFORMATION

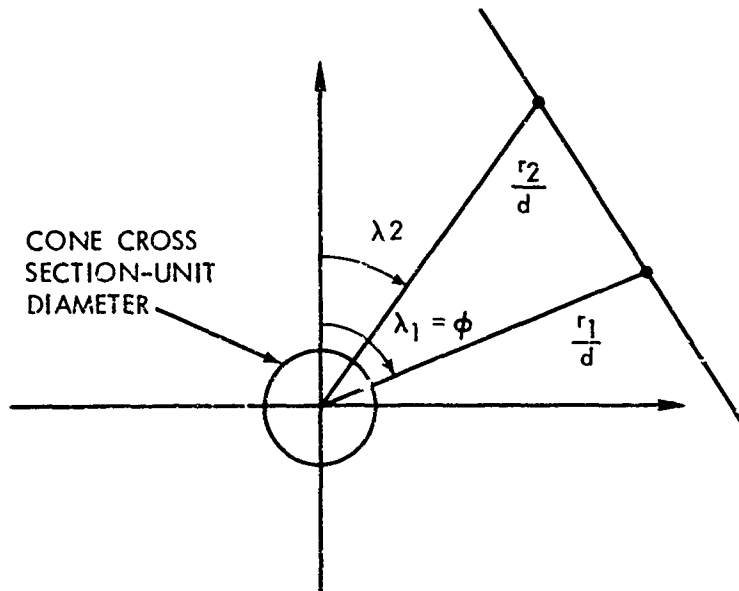


FIG. 10 CONSTRUCTION OF "EFFECTIVE LINE OF SITE" IN POLAR CROSS-SECTIONAL PLANE



FIG. 11a SCHLIEREN PHOTOGRAPH OF A 5° HALF ANGLE CONE AT ANGLE OF ATTACK
 $\alpha = 15^\circ, \phi = 0^\circ$

NOLTR 69-80



FIG. 11b $\phi = 60^\circ$

NOLTR 69-80

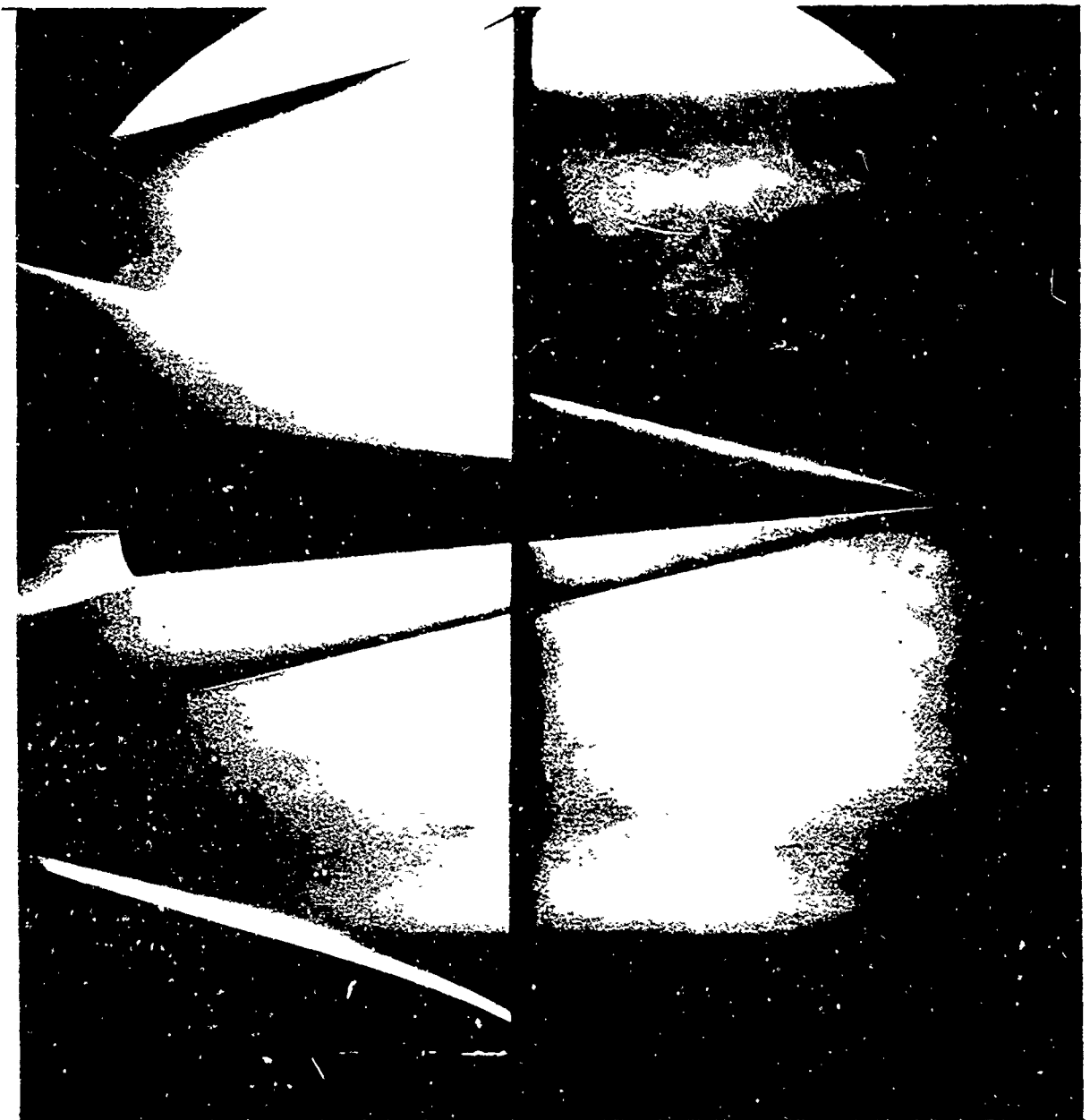


FIG. 11c $\phi = 90^\circ$

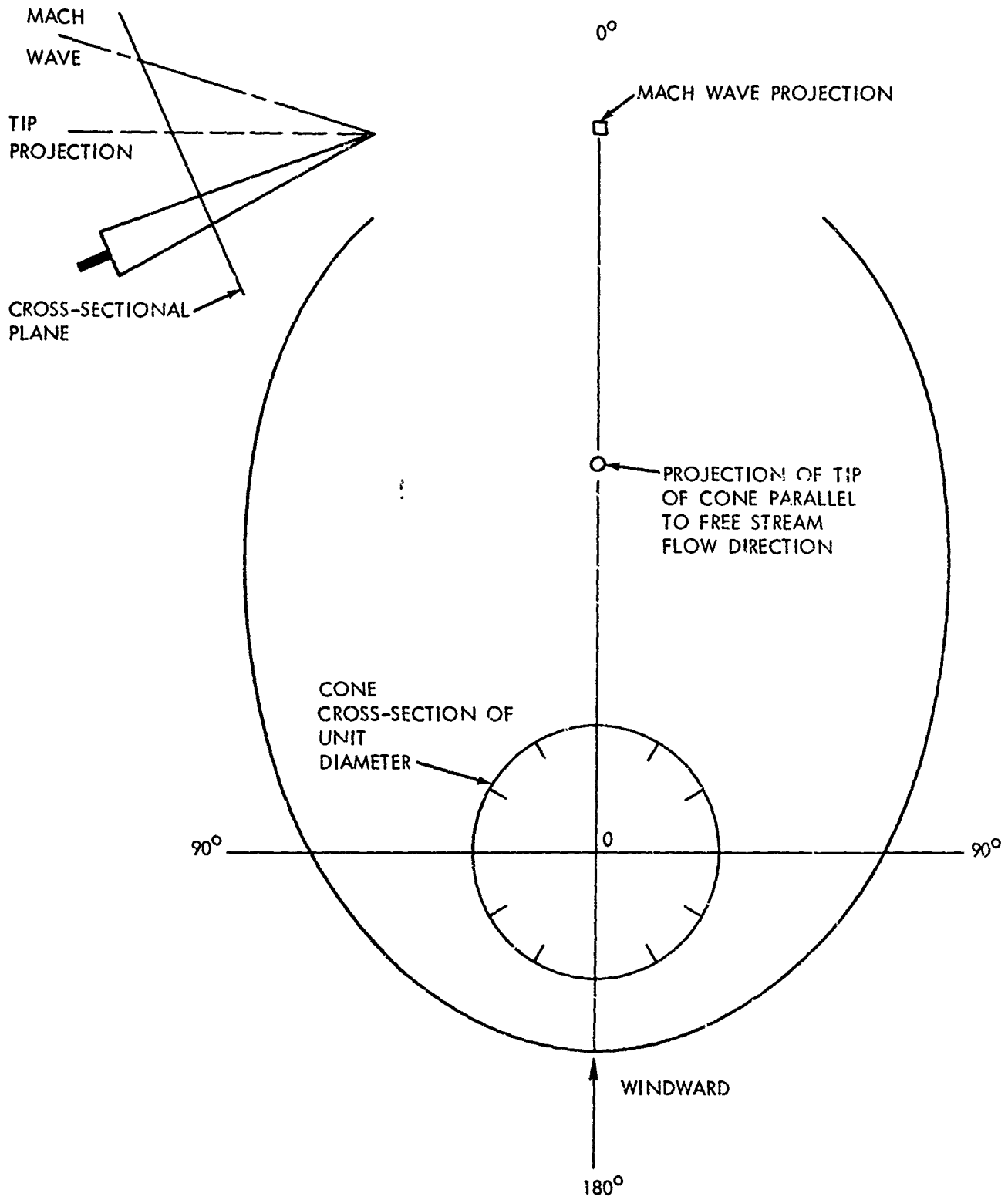


FIG. 12 SHOCK WAVE PROFILE OF RIGHT CIRCULAR CONE AT ANGLE OF ATTACK $\alpha = 15^\circ$

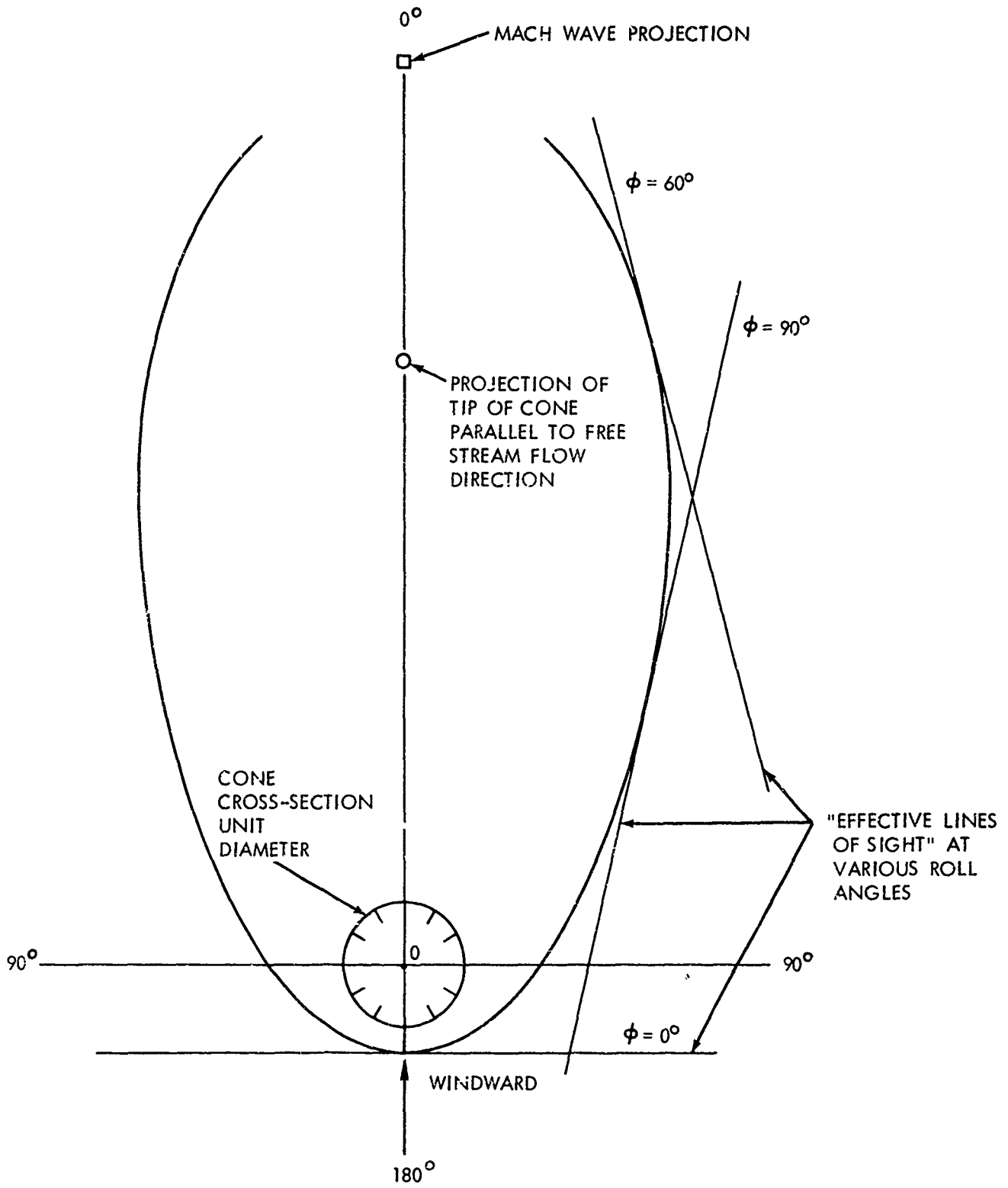


FIG. 13 SHOCK WAVE PROFILE OF RIGHT CIRCULAR CONE AT ANGLE OF ATTACK $\alpha = 40^\circ$

DOCUMENT CONTROL DATA - R & D

Security classification of title, body of abstract and indexing annotation must be entered when the overall report is classified

1 ORIGINATING ACTIVITY (Corporate author)		2a. REPORT SECURITY CLASSIFICATION	
U. S. Naval Ordnance Laboratory White Oak, Silver Spring, Maryland		UNCLASSIFIED	
		2b. GROUP	
3 REPORT TITLE			
How to Analyze 2-D Schlieren Photographs to Obtain the Density Gradient Structure of 3-D Flow Fields			
4 DESCRIPTIVE NOTES (Type of report and inclusive dates)			
final			
5 AUTHOR(S) (First name, middle initial, last name)			
Allen E. Winkelmann and Robert H. Feldhuhn			
6 REPORT DATE	7a. TOTAL NO OF PAGES	7b. NO OF REFS	
15 April 1969	15 plus illus.	2	
8a. CONTRACT OR GRANT NO	9a. ORIGINATOR'S REPORT NUMBER(S)		
b. PROJECT NO	NOLTR 69-80		
c.	9b. OTHER REPORT NO(S) (Any other numbers that may be assigned this report)		
d.			
10 DISTRIBUTION STATEMENT			
This document has been approved for public release and sale, its distribution is unlimited.			
11 SUPPLEMENTARY NOTES		12 SPONSORING MILITARY ACTIVITY	
13 ABSTRACT			
<p>A technique is outlined by which density gradients visible in two-dimensional schlieren photographs can be analyzed to obtain the density gradient structure (i.e., the shape and location of density gradients such as shock waves and vortices) of three-dimensional flow fields. Practical application of the technique relies on obtaining a series of schlieren photographs of the flow field from different viewing orientations. The analysis is specialized to the case of a right-circular cone at angle of attack. Results are presented which show the shape and location of the bow shock of a 5° half-angle right-circular cone tested in the Supersonic Tunnel No. 2 at the U. S. Naval Ordnance Laboratory, White Oak, at a nominal Mach number of 5.0, a nominal free-stream Reynolds number per foot of 4.8×10^6 and angles of attack equal to 15° and 40°.</p>			

14 KEY WORDS	LINK A		LINK B		LINK C	
	ROLE	WT	ROLE	WT	ROLE	WT
Flow visualization schlieren flow-field surveys density gradients						